https://doi.org/10.5194/essd-2025-739
Preprint. Discussion started: 29 December 2025

Open Access Earth System Science Data Discussions

Unveiling the Deep Ocean warming: observed bottom ocean dataset across Mediterranean Sea

Nadia Lo Bue[1], Beatrice Giambenedetti[1], Davide Embriaco[2], Paolo Bagiacchi[1], Claudia Fratianni[3], Riccardo Vagni[2], Giuditta Marinaro[1].

[1]Istituto Nazionale di Geofisica e Vulcanologia (INGV), Via di Vigna Murata 605, 00143 Rome, Italy

[2]Istituto Nazionale di Geofisica e Vulcanologia (INGV), Via S. Teresa, Pozzuolo 19032 Lerici (SP), Italy

[3]Istituto Nazionale di Geofisica e Vulcanologia (INGV), Viale Berti Pichat 6/2, 40127 Bologne, Italy

Correspondence to: Nadia Lo Bue (nadia.lobue@ingv.it)

Abstract

The deep ocean was long assumed to be in a quasi-stationary state, and therefore excluded from studies on climate variability. The awareness of the unsteady state of the deep ocean is a fairly recent achievement, but despite its pivotal role in the assessment of climate variability, the understanding of abyssal ocean dynamics remains largely unknown, primarily due to the scarcity of observations. This is why any observations below 2000 meters depth, although poor or widely dispersed, constitute valuable knowledge that is mandatory to enhance and make available.
This work presents validated oceanographic time series collected by benthic multidisciplinary observatories across key locations in the Mediterranean Sea region. It includes details on the data processing and quality control methods used to ensure reliability and aims to deliver high-quality data, as well as standardization in the quality control procedures for deep-sea measurements.
The dataset provides a comprehensive description of seafloor observations collected over different time periods during the past decade, contributing to the long-term characterization and understanding of abyssal ocean variability in the region.

Short Summary

We present a set of long-term, high-resolution oceanographic datasets collected by benthic observatories across the deep Mediterranean Sea. These datasets provide valuable insight in the study of deep ocean dynamics and its possible impact on climate variability. By applying standardized post-processing and quality control procedures, we ensure the data's reliability and usability for further analysis and model

https://doi.org/10.5194/essd-2025-739
Preprint. Discussion started: 29 December 2025

validation. This contribution addresses critical gaps in deep-sea monitoring and supports efforts aligned with the UN Decade of Ocean Science.

1 Introduction

The deep ocean is the largest, yet least observed, component of the Earth's climate system. For decades, it was assumed to be a quasi-stationary environment (*Stommel and Arons, 1960; Munk, 1966*) and thus was largely excluded from global monitoring strategies. The unsteady state of the deep ocean is a quite new achieved knowledge (*Ferrari et al. 2016, MacKinnon et al, 2017, Polzin and McDougall, 2011*) that emphasizes the significance of abyssal processes in redistributing heat and energy, thereby influencing surface climate variability.

Recent findings (*Talley et al 2016., Desbruyères et al. 2016, Artale et al., 2018*) show that, all over, the deep ocean is far from being a stable environment; rather, it is an active part of the climate system, exerting measurable impacts on decadal time scales. The deep sea is indeed a highly complex and interconnected environment. The whole water column is in continuous vertical exchange up to the surface and with the atmosphere, as well as laterally with surrounding ocean basins, guided by morphological constraints. Given the crucial role of the oceans in absorbing planetary energy imbalance (93%) (*Rhein et al., 2013*), understanding how and on what timescale deep-water masses redistribute this energy is essential for assessing long-term climate variability and ocean circulation dynamics (*Lo Bue et al., 2021*). Deep sea variability and the impacts of climate change on it are difficult to interpret, and it is difficult to disentangle the different contributions given the small number of available observations, as well as discriminate between local variability and climate change. These knowledge gaps are reflected in current global climate models, where abyssal processes are not well-represented, leading to important biases in the global climate variation estimates. Global climate models need observations for model design, tuning, and validation, so it is straightforward that the under-observed deep ocean results in being poorly represented (*Heuzè et al. 2022)*. Recognition of observation as a critical element for ocean health and planet sustainability boosted observing efforts since 2000, but this has almost exclusively concerned the surface ocean *(Visbeck, 2018)*. Therefore, the capacity to comprehend and quantify the energy redistribution in the deep ocean and its effects on climate variability will remain underestimated until enhancements in systematic monitoring across a substantial volume of (deep) ocean are achieved. Despite the development of several global ocean observing programs over the past decade, such as ARGO, OceanSITES, GO-SHIP, OOI, ONC, and EMSO, providing continuous deep ocean monitoring, they still only cover a limited and scattered portion of the vast ocean (*Levin et al. 2019*). Currently, just 6% of

https://doi.org/10.5194/essd-2025-739
Preprint. Discussion started: 29 December 2025

hydrographic observations extend below 2100 m in depth (*de Lavergne et al. 2016*), while the global mean ocean depth exceeds 4000 m.

As suggested by the UN decade (Howell, 2021), there is an urgent need to fill the knowledge gap about the deep ocean. This requires a collaborative, synergistic effort that places priority on enhancing observation networks and monitoring programs across various domains as well as delivering standardized, high-quality datasets to support both process studies and model development. High-resolution, long-term datasets are essential not only for understanding deep ocean variability but also for reducing biases in global climate models, which currently lack robust parameterizations for abyssal processes (Heuzé et al., 2022).

In this context, we present a collection of validated, long-term oceanographic datasets acquired by benthic observatories deployed at key sites across the deep Mediterranean Sea. These observatories provide unique data for sampling strategies, heterogeneity, location, and endurance. The aim is to facilitate knowledge sharing and promote a harmonized approach to deep-sea monitoring that supports broader scientific efforts in climate research, model validation, and new ocean insight.

2 Data acquisition system

Accurate and continuous deep-sea monitoring requires advanced data acquisition systems capable of withstanding extreme conditions and capturing a broad range of environmental variables over extended periods. In this sense, benthic multidisciplinary observatories, such as GEOSTAR-type system (Favali et al. 2006; Favali et al., 2009, Favali et al., 2013) (Fig. 1), are essential tools, integrating physical, chemical, and geophysical sensors to acquire high-resolution data in challenging deep-ocean conditions, where pressure, oxidation and temperature can affect the functioning of the system itself.

Benthic observatories can be broadly categorized into two types: autonomous (standalone) and cabled systems. The choice between these configurations depends on monitoring objectives, site accessibility, power and data requirements and logistical constraints.

Autonomous systems are designed to operate without external power or data transmission infrastructure. Powered by onboard lithium batteries, these systems store data locally until physical recovery. Low-power electronics are used to optimize battery life, and sensor data are timestamped using high-precision rubidium clocks and stored in a central internal memory. Special attention is paid to sensor placement to minimize interference from the frame structure and to ensure optimal sampling conditions. Depending on the mission configuration, autonomous systems can operate for periods up to one year (*Embriaco et al., 2014; Marinaro et al., 2006; Favali et al., 2006; Beranzoli et al., 1998*). The autonomous nature of these systems makes them particularly valuable for deployments in remote areas where establishing a

https://doi.org/10.5194/essd-2025-739
Preprint. Discussion started: 29 December 2025

continuous power or data connection is impractical. However, their reliance on limited battery life and local data storage means that they require periodic recovery and maintenance, limiting their ability to provide real-time data.

Figure 1: Example of a GEOSTAR-type observatory integrating multidisciplinary sensors. The image shows the NEMO-SN1 benthic observatory during the GNDT-1 campaign (2002–2003).

Cabled observatories, by contrast, are connected to shore stations via electro-optical submarine cables, allowing for real-time data transmission and continuous power supply. A cabled observatory such as NEMO-SN1(*Favali et al., 2013, Giovannetti et al.,2016*) incorporates an electro-optical jumper and a 28 km-long submarine cable that connects the system to a dedicated onshore acquisition system. This setup enables uninterrupted data collection, remote control of sensors, and real and near-real-time quality control (depending on the type of data acquired). Time synchronization is achieved via a GPS signal received at the shore station, ensuring high temporal accuracy across all measurements. Cabled systems are ideal for deep long-term monitoring in accessible regions requiring high-frequency, real-time data. Table 1 summarizes the observatories, deployment sites, and sensor configurations described in this study.

https://doi.org/10.5194/essd-2025-739
Preprint. Discussion started: 29 December 2025

3 Dataset, processing, and quality control

Monitoring the deep sea presents significant challenges, from instrument deployment and data recovery to ensuring the accuracy, quality and comparability of measurements, primarily due to its remote and extreme environment. Harsh environmental conditions, logistical complexity, and technological variability across observatories result in heterogeneous datasets requiring robust processing and harmonization. This section outlines the datasets, their characteristics, and the quality assurance (QA), the standardized post-processing, and quality control (QC) procedures adopted to enhance data integrity, reliability, and interoperability.

3.1 Datasets

Between 2002 and 2014, eight long-term multidisciplinary time series were collected by four different benthic observatories strategically located across the Mediterranean Sea (Fig. 2). Each observatory hosts a wide array of geophysical sensors. However, for the purposes of this paper, we focus only on those measuring physical and biogeochemical parameters, notably: temperature, conductivity, pressure, turbidity, and ocean currents. Sensor operation varied across deployments, with sampling intervals depending on the sensor type and mission objectives. A central data acquisition unit guarantees time synchronization among sensors that operate with different sampling intervals, ranging from hourly to a frequency as high as 5 Hz. Table 1 provides a summary of each observatory, including deployment periods, sensor types and models, sampling frequencies, and overall data acquisition efficiency. Below, we present a detailed description of the datasets acquired at each site.

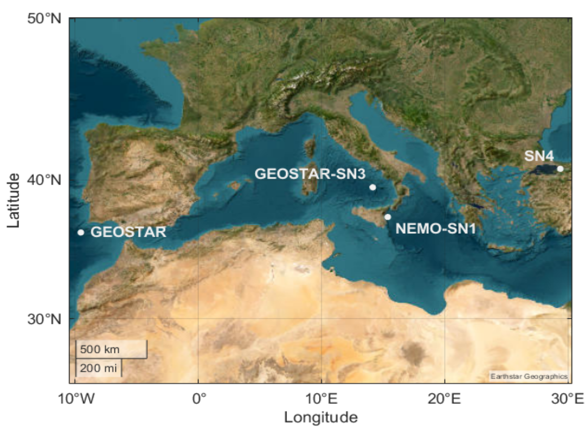

Figure 2: Location of the benthic multidisciplinary observatories: GEOSTAR (Gulf of Cadiz), GEOSTAR-SN3 (Tyrrhenian Sea), NEMO-SN1 (Ionian Sea), and SN4 (Marmara Sea), (© *2025 Google Earth*).

https://doi.org/10.5194/essd-2025-739
Preprint. Discussion started: 29 December 2025

NEMO-SN1 observatory (Western Ionian Sea, 2100 m), located ~25 km off the coast of Eastern Sicily (37.5° N, 15.4° E), yielded two different monitoring campaigns: October 2002–February 2003 and June 2012–June 2013 (*Favali et al. 2006*, *Favali et al. 2011, Favali et al. 2013*). The first deployment included a CTD probe (SBE 37SM) sampling every 12 minutes, and an acoustic punctual current meter (Falmouth 3D-ACM) operating at 2 Hz. This sensor payload was then improved for the second campaign (2012-2013) by adding an ADCP (RDI WorkHorse, 600kHz), sampling current profiles every 30 minutes. Also, a new punctual acoustic current meter (Nobska MAVS-3 3-axis) replaced the previous one, maintaining the same sampling frequency, while the sampling rate of the CTD was changed to 1 sample per hour. This site is a key transition zone for water mass exchange between the Levantine Basin, Adriatic Sea, and Western Mediterranean, and plays a central role in deep thermohaline circulation of the Eastern Mediterranean (*Malanotte-Rizzoli et al., 1997; Lascaratos et al., 1999; Gacic et al., 2010, Budillon et al. 2010*).

GEOSTAR-SN3 (Southern Tyrrhenian Sea, 3320 m), located on the Marsili abyssal plain (39.5° N, 14.2° E), GEOSTAR-SN3 represents the first long-term pilot deployment at this site. This observatory was implemented to act as the main node of an underwater network of deep-sea observatories (*Favali et al. 2009*). It operated in two consecutive missions: 2003–2004 and 2004–2005. The observatory was equipped with a CTD (SBE 16plus), a transmissometer (Chelsea Alphatracka II), an ADCP (RDI WorkHorse 300 kHz), and a point current meter (Falmouth 3D-ACM), all sampling at hourly intervals, except for the last sensor that operated at 2 Hz. Due to the presence of the Marsili Volcano, which represents one of the largest European underwater volcanoes of the Plio-Pleistocenic age, this area is key for addressing both geophysical and oceanographic topics (*Beranzoli et al. 2009*).

GEOSTAR (Gulf of Cadiz, Iberian Sea, 3200 m), an updated version of the GEOSTAR seafloor observatory, was then deployed between 2007 and 2010 near shore in the Gulf of Cadiz (Iberian Sea - 36.4°N, 9.5°W). This deployment was part of the CE NEAREST project (Integrated observation from NEAR shore sourcES of Tsunami: Towards an early warning system) (*Favali et al. 2009*), which aimed to enhance the near-real-time detection of signals through a multiparameter seafloor observatory designed to characterize potential sources of tsunamis, contributing to the development of a prototype Early Warning System (EWS). From an oceanographic perspective, this site is significant for monitoring interaction between the North Atlantic current and the Mediterranean outflow, contributing to the oceanographic characterization of a key interbasin exchange zone *(Alves et al. 2011, García-Lafuente et al. 2006, Ochoa et al. 1991*). The sensor suite included a CTD (SBE 16plus), a turbidimeter (Wet Labs

https://doi.org/10.5194/essd-2025-739
Preprint. Discussion started: 29 December 2025

ECO BB), an ADCP (RDI WorkHorse 300 kHz) sampling every 10 minutes and a punctual current meter (Nobska MAVS-3) sampling at 5 Hz.

SN4 (Marmara Sea, 166 m)**,** deployed along the North Anatolian Fault in the Gulf of Izmit (40.7° N, 29.4° E), SN4 monitored seismic activity and its coupling with environmental parameters. Campaigns were conducted in 2009–2010 and 2013–2014, with durations of 5 and 7 months, respectively. Although SN4 is one of the smallest GEOSTAR-class observatories, its instrumentation includes both geophysical and oceanographic sensors *(Favali et al. 2009, Marinaro et al. 2006*), hosting CTD (SBE 16plus), a turbidimeter (Wet Labs ECO NTU), an oxygen optode (AADI 3830), and a point current meter (Nobska MAVS-3), with sampling frequencies ranging from 1 sample every 10 minutes (CTD, turbidity) to 1 Hz (oxygen) and 5 Hz (currents). The observatory's purpose is to investigate potential correlations between seismic activity and gas methane emissions in the surrounding environment, given the area's status as an active seismic zone (*Embriaco et al., 2014*).

3.2 post-processing and quality control

The long-term deployment of observatories, along with the evolution of instrumentation over the years, has resulted in variability in data formats and metadata structures. Consequently, a tailored post-processing procedure for each observatory was required to face these discrepancies. To provide a more reliable comparison for future dissemination and usage of the data, in compliance with the FAIR (Findable, Accessible, Interoperable, and Reusable) principles for data sharing, the post-processing workflow consisted of several steps: converting raw data into usable formats, harmonizing metadata, and applying quality checks. Preliminary analysis was always conducted, as the first step, to evaluate the data storage efficiency (Table 1). The raw data extracted from the deck unit were converted into a readable format using custom-designed software tailored for each specific observatory, whereas certain types of data, such as ADCP data, required conversion using the manufacturer's software. Each dataset underwent post-processing utilizing specific multi-step standardized procedures following the manufacturer's recommendation. This process enhances the accuracy, reliability, and interpretability of the raw data, refining its quality and facilitating better interpretation. The QC procedures were guided by recommendations from international frameworks such as GOOS (*IOC, 2010; Pouliquen et al., 2011*) and QUARTOD (*Bushnell et al., 2019*). Tests included checks for time consistency, value ranges, rate of change, and internal consistency across sensors. Data were flagged based on severity and usability (Table 2), with bad or missing data replaced by NaNs to maintain data integrity.

https://doi.org/10.5194/essd-2025-739
Preprint. Discussion started: 29 December 2025

Table 1: Overview of the benthic observatories, including site location, deployment period, sensor types and models, sampling frequency, and acquisition efficiency.

Observatory name, depth, and geographical site	Acquisition period	Sensor type	Sensor model	Sampling frequency	Sensor efficiency (%)
NEMO-SN1 (2100 m) Western Ionian Sea	2002-2003 and 2012-2013	CTD	SBE 37 SM	1 sample/12'	100% (2002-2003) 95.3% (2012-2013)
		CURRENT METER	Falmouth 3D-ACM (2002-2003) Nobska MAVS-3 (2012-2013)	2Hz	99.9% (2002-2003) 98.4% (2012-2013)
		ADCP	RDI WH 600 kHz	2 samples/h	98.7% (2012-2013)
GEOSTAR SN3 (3320m) South Tyrrhenian Sea	2003-2004 and 2004-2005	CTD	SBE 37 SM	1 sample/h	99.5% (2003-2004) 98.5% (2004-2005)
		TRANSMISSOMETER	Chelsea Alphatracka II	1 sample/h	99.5% (2003-2004) 98.5% (2004-2005)
		CURRENT METER	Falmouth 3D-ACM	2Hz	100% (2003-2004) 99.9% (2004-2005)
		ADCP	RDI WH 300 kHz	1 samples/h	100% (2003-2004) 99.7%(2004-2005)
GEOSTAR (3200) Gulf od Cadiz	2007-2008 and 2009-2010	CTD	SBE16plus	1 samples/h	91.4% (2007-2008) 96.1% (2009-2010)
		TURBIDIMETER	Wet Labs ECO BB	1 samples/h	91.4% (2007-2008) 96.1% (2009-2010)
		CURRENT METER	Nobska MAVS-3	5Hz	90.5%(2007-2008) 36.8%(2009-2010)
		ADCP	RDI WH 300 kHz	1 sample/h	90.5% (2007-2008) 36.8% (2009-2010)
SN4 (166 m) Marmara Sea	2009-2010 and 2013-2014	CTD	SBE16plus	1 sample/10'	99.5% (2009-2010) 99.7% (2013-2014)
		TURBIDIMETER	Wet Labs ECO BB	1 sample/10'	99.5% (2009-2010) 99.7% (2013-2014)
		CURRENT METER	Nobska MAVS-3	5Hz	99.9% (2009-2010) 17.7% (2013-2014)
		OXYGEN	AADI Optode 3830	1 Hz	99.9% (2009-2010)

3.2.1 post-processing

The first stage aimed to collect, convert, and verify the data gathered by different acquisition systems, considering the diverse types of sensors and the relative data format, to enhance the quality and reliability of the collected information. A thorough post-processing phase was undertaken to refine and further validate the data. This involved primarily an inspection of the efficiency of the sensors and their proper functioning through meticulous post-calibration and validation procedures to ensure the integrity of the

https://doi.org/10.5194/essd-2025-739
Preprint. Discussion started: 29 December 2025

data, providing a solid foundation for subsequent analysis and interpretation. Table 1 reports the efficiency for each sensor and mission elaborated, where the overall acquisition efficiency is calculated as the percentage of data recorded on the total acquisition load. The efficiency of the oceanographic sensors was generally very high, with a few exceptions, most notably in the Marmara Sea (Table 2), where the Nobska MAVS-3 sensor stopped functioning relatively early in the mission. Subsequently, several checks were performed to verify timestamp validity, ensure alignment of multivariable measurements, and assess instrument efficiency.

Table 2: Definitions of quality flags applied to datasets. Missing and Bad data (flag 9) are not retained and replaced in the new QC datasets with NaNs.

Code	Definition
1	Good data
3	Suspect data potentially correctable or high-interest data
9	Missing value or bad data

Moreover, cross-correlation techniques were employed to verify internal consistency, particularly between current meters and ADCPs. For instance, the horizontal velocity component (U) measured by the punctual current meter and by the ADCP deployed at GEOSTAR-SN3 during the 2003-2004 mission showed reasonable agreement ($R^2 = 0.28$), as illustrated in Figure 3.

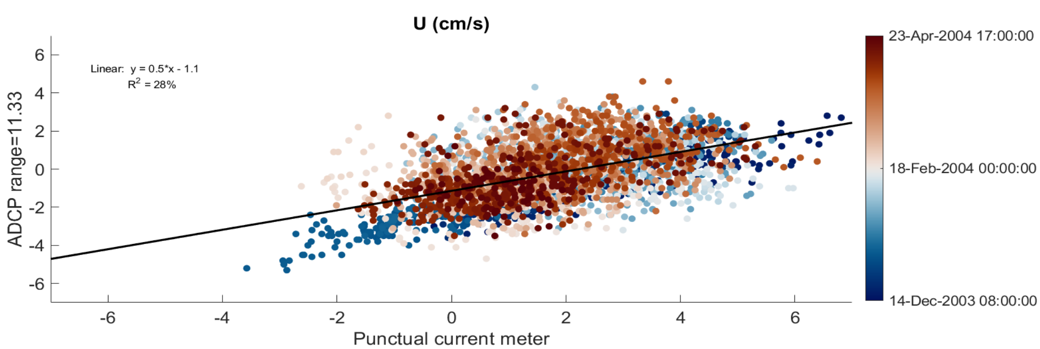

Figure 3: Comparison of the horizontal (U) velocity components from punctual current meter and ADCP at GEOSTAR-SN3 (2003–2004). To match these two different types of data we considered the hourly time series.

https://doi.org/10.5194/essd-2025-739
Preprint. Discussion started: 29 December 2025

This consistency was observed despite differences in their operating principle, measurement accuracy and installation height. The ADCP profiles a section of the water column above the observatory (up to 20 – 30 m in this example), while the punctual current meter captures velocity closes to the sensor itself, close to the bottom. This comparison helps confirm the reliability of the collected data.

3.2.2 Quality Control Procedures

Before any QC procedure can be meaningfully applied, however, rigorous Quality Assurance (QA) is essential to ensure that the sensors themselves provide measurements within expected accuracy and stability ranges. In these cases, QA included pre-deployment sensor calibration and in situ verification through dedicated CTD casts conducted both immediately before the observatory deployment and after recovery. These steps establish the baseline performance of each instrument, allow the identification of sensor drift or malfunction. Ensuring robust QA is fundamental, as even the most sophisticated QC procedures cannot fully compensate for poorly calibrated or improperly functioning sensors; rather, effective QA provides the foundation upon which reliable real-time and delayed-mode QC can be built. Whether performed in real-time or in delayed mode, QC data is crucial for ensuring the accuracy, reliability, and consistency of the data collected. For cabled observing systems, real-time QC serves as an invaluable tool for assessing, monitoring sensor performance and developing possible real-time applications. It also helps prevent the storage and analysis of erroneous data, while enabling prompt corrections that can minimize data gaps or inaccuracies during critical monitoring periods.

In contrast, delayed mode QC provides a more comprehensive review to improve data accuracy. It involves comparing measurements with reference datasets, historical records, or model outputs, allowing the detection and correction of errors missed during real-time processing. Sensor recalibration and cross-referencing with nearby instruments are commonly applied. By applying advanced statistical and tailored threshold-based techniques (e.g. range tests, spike and outlier detection), together with time series methods (e.g. low-pass/high-pass filtering, trend analysis, autocorrelation), delayed mode QC can effectively address issues such as missing data, spikes, and sensor drift, thereby substantially enhancing overall data quality. Since deep ocean data is often collected over extended periods, delayed mode QC plays a crucial role in identifying and correcting inconsistencies caused by sensor degradation or calibration drift. This is especially important for long-term environmental studies, where maintaining consistency across datasets is essential for reliable trend analysis and meaningful comparisons.

https://doi.org/10.5194/essd-2025-739
Preprint. Discussion started: 29 December 2025

All datasets here described, whether collected through stand-alone or cabled system, have been processed in delayed mode with the aim of archiving the dataset for long-term use and sharing high-quality data with the scientific community.
Following QUARTOD (QA/QC for Real-Time Oceanographic Data) recommendations (*Pouliquen et al. 2011*), a QC protocol was customized for each sensor type and designed to be as automated as possible. Data that failed one or more tests were either flagged or removed according to the test rules. Missing or bad (removed) data were substituted with NaNs, while preserving their corresponding timestamps to maintain a regular temporal grid in the dataset. Custom thresholds were defined for regional and seasonal variability based on climatological data from the Mediterranean Sea (Table 3).

Table 3: Example of regional thresholds used in quality control tests for the Mediterranean Sea, including seasonal and climatological variability.

SITE	VARIABLE	RANGE
Ionian Sea and TyrrhenianSea	Temperature	13-14° C
	Conductivity	4-5 S/m
	Current Speed	0-20 cm s^{-1}
Marmara Sea	Temperature	14-16° C
	Conductivity	4-5 S/m
	Current Speed	0-40 cm s^{-1}
Cadiz Gulf	Temperature	2-3° C
	Conductivity	2-4 S/m
	Current Speed	0-20 cm s^{-1}

These measures ensured that flagged data reflected real anomalies rather than environmental variability. Figure 4 provides an overview of the quality of the seafloor observatory data after applying the post-processing and the QC procedure using flags defined in Table 2.

https://doi.org/10.5194/essd-2025-739
Preprint. Discussion started: 29 December 2025

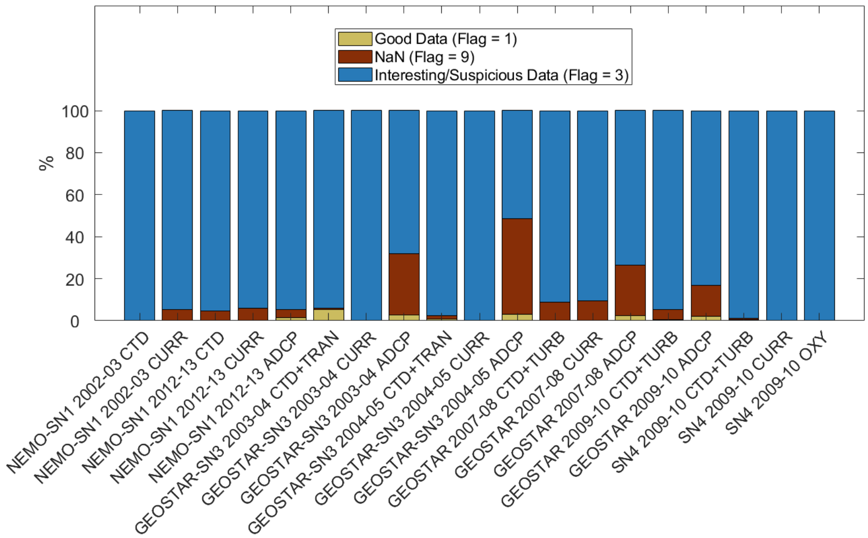

Figure 4: Data quality distribution across observatories and sensors after QC. Data quality flags as percentages for all processed datasets. Bars indicate observatory name, campaign years, and sensor type. Flag codes: 1 = good, 3 = suspect, 9 = missing/removed

The QC procedure was carried out through a stepwise sequence of tests, such as:

Time check - The test concerns missing timestamps requires that the observation date and time are sensible and cover the whole campaign duration with the frequency of the instrument. Missing data are typically detected and flagged. In some cases, the acquisition system automatically inserts a standard out-of-range value (e.g., '999') in the raw data to indicate a malfunction; these values are identified and replaced with NaNs.

Out of range test - Removing any measurements that exceed the output-range thresholds assigned individually to each sensor

Gross Range test - The global range test evaluates each observed value against the full spectrum of physically plausible measurements, encompassing both the extreme conditions expected in the oceans and the operational limits of the sensors. Any value that falls outside this predefined range is automatically flagged or removed, ensuring that clearly erroneous measurements are excluded from subsequent analyses.

Percent Good (ADCP only) - This test uses the beams' percent good, which indicates what fraction of the pings were accepted for a given ensemble. The percent good test determines whether the data that are being returned are sufficient to provide the required data quality. For Teledyne RDI ADCPs, when the coordinate frame is not set to beam coordinates, the Percent Good test applies to the percentage of good three and four beam solutions, i.e., the percentage of data for which the sensor has rejected none or only one beam.

Error velocity test (ADCP only) - Uses error velocity, which derives from the four-beam geometry of an ADCP, each pair of opposing beams providing two independent measurements of velocity. The error velocity can be treated as an indicator of errors for each depth bin. Threshold specification from the sensor manufacturer.

Regional/Seasonal range test - This is a variation on the gross range test, where the thresholds are adjusted to seasonal averages (e.g., climatological ranges, expected variability from the measured region). Table 4 provides an example of specific ranges for observations from the Mediterranean Sea.

Spike test - This test checks for single value spikes usually due to an electrical signal from the sensor, relative to adjacent data points. Spikes consisting of more than one data point are difficult to capture, but their onset may be flagged by the following Rate of change test.

Rate of change – This test inspects the time series for a time rate of change that exceeds a threshold. The observed quantities can change substantially over short periods in some locations, hindering the value of this test, so the thresholds have been chosen carefully and tailored based on the sensor's operational limits and location. This test is equivalent to removing outliers, i.e. data over three standard deviations from the mean. In the case of dissolved oxygen measurements, because of its dynamic nature, this test does not involve outliers' removal but flagging.

Flat line - A common sensor failure mode can provide a data series that is nearly a flat line suggesting sensor failure. This test checks for a continuously repeated observation of the same value. Since in the deep sea there is generally little variability, this kind of test is performed for flagging suspicious data since it cannot be considered necessarily bad in this specific case.

Sensor Tilt (for current meter and ADCP) - Current sensors must be aligned within an expected range of tilt angles to properly measure horizontal and vertical currents. For fixed-mounted sensors, as in the case of seafloor observatories, this test serves to verify that there has not been a misalignment or an unexpected platform motion in time. In the case of ADCP measurements, this test can be replaced with a rate of change test performed along the vertical (i.e., along depth instead of time).

https://doi.org/10.5194/essd-2025-739
Preprint. Discussion started: 29 December 2025

Echo Intensity (ADCP only) - If a beam reflects off a boundary, then the echo intensity increases from the previous bin. The test checks for echo intensities that may indicate interaction with the surface, bottom, or in-water structures.

Current gradient (ADCP only) - The current speed is expected to change at a gradual rate with depth. This test checks for excessive current speed/direction changes in the vertical profile.

An example of the QC procedure is shown in Figure 5, using the horizontal velocity component measured by the punctual current meter on GEOSTAR-SN3 during the 2003–2004 mission. The raw data initially contained numerous spikes, out-of-range values, and outliers, making interpretation difficult (Figure 5a). Applying only the out-of-range test significantly improved data clarity (Figure 5b) and completing the full QC process resulted in a clean and accurate representation of the eastward velocity component (Figure 5c). All tests were conducted within the valid measurement range for the instrument, as specified in Table 4. These QC procedures, excluding the tilt test, were also applied to CTD probes, turbidimeters, and transmissometers. For CTD data, derived quantities were calculated using the international TEOS-10 (*Thermodynamic Equation of SeaWater, 2010*) subroutines (*McDougall and Barker, 2011*), including in-situ salinity (S, PSU), absolute salinity (SA, g/kg), conservative temperature (CT, °C), potential temperature (θ, °C), and in-situ density (ρ, kg/m^3).

For dissolved oxygen measurements, the same QC procedures were used, with a modified rate-of-change test to account for the dynamic nature of oxygen in the marine environment.

The ADCP measurements required a slightly different approach compared to the other sensors due to their operational differences. Figure 6 shows an example of the QC steps applied to the velocity magnitude measured by the ADCP mounted on SN3 observatory during the 2003-2004 acquisition campaign.

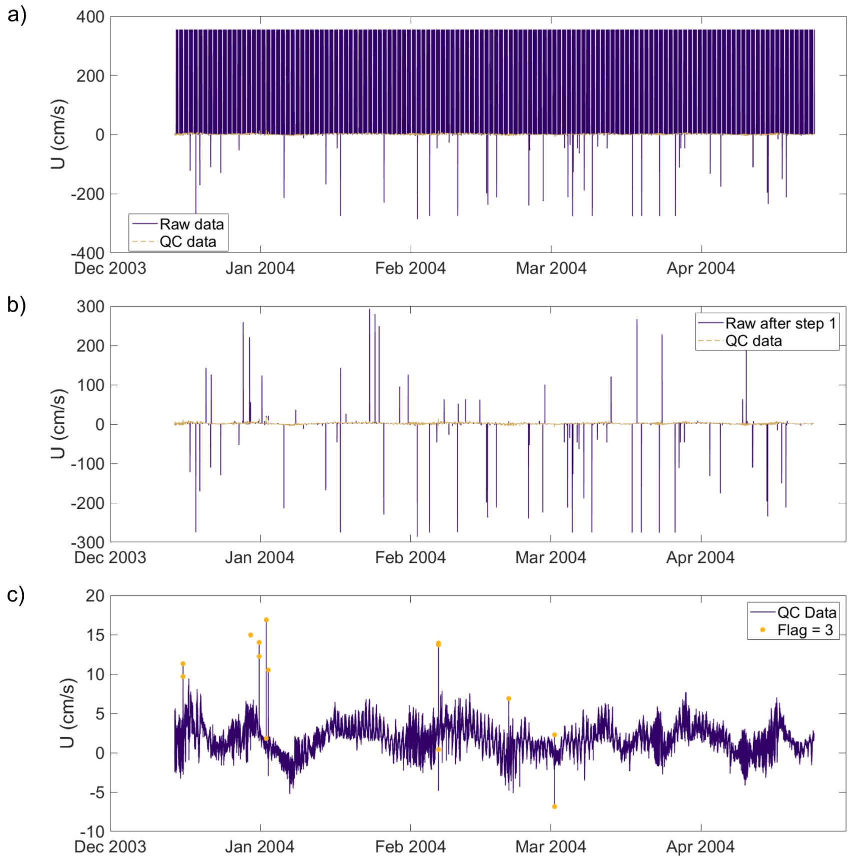

Figure 5: Quality control procedure applied to the eastward velocity component measured by the punctual current meter at GEOSTAR-SN3 (2003–2004). (a) Raw data showing outliers; (b) intermediate results after range and spike tests; (c) final cleaned dataset after applying full QC protocol.

This sensor measures current time series across various depth ranges, up to ~20 m from the top of the observatory. Consequently, visual inspection of the raw dataset is more difficult to interpret, as can be seen in Figure 6(a), noisy data is not immediately evident in the raw data. The two panels of Figure 6(a) have been limited to a single month to better highlight the differences between the raw and the quality checked data, particularly in the upper ranges where the measurements are noisier. Figure 6(b) displays detailed data extracted from two different depths at 5.33 and 20.33 m above the sensor, highlighting more clearly the effects of the QC procedures. Each depth range is tested for ranges, spikes, outliers, flat lines, and tilt, like the other sensors. Additionally, the rate of change in the vertical direction, the percentage of data acquired using three or more beams, echo intensities to account for spurious ping interactions, and the velocity error range are also evaluated.

https://doi.org/10.5194/essd-2025-739
Preprint. Discussion started: 29 December 2025

Open Access Earth System Science Data Discussions

Table 4: Statistical parameters computed for time series from all observatories, including sensor type and campaign details.

Observatory name	Acquisition campaign	Sensor	Variable	Minimum	Maximum	Mean	Standard deviation
NEMO-SN1	2002-2003	CTD	T (°C)	13,71	13,77	13,75	0,01
			C (S/m)	4,648	4,656	4,652	0,001
			Depth (dbar)	2102,8	2110,7	2109,7	1,8
		Current meter	U (cm/s)	-17,7	10,8	-2	1,9
			V (cm/s)	-5,2	24	7,8	3
			W (cm/s)	-12,5	20,2	-0,6	1
	2012-2013	CTD	T (°C)	13,74	13,82	13,76	0,02
			C (S/m)	4,656	4,665	4,658	0,002
			Depth (dbar)	2060,1	2060,8	2060,5	0,1
		Current meter	U (cm/s)	-12,1	8,9	-1,4	1,4
			V (cm/s)	-15,9	7,1	-3	1,9
			W (cm/s)	-7,4	7,8	0,5	0,6
		ADCP	U (cm/s)	-19,9	20	-2	3
			V (cm/s)	-19,9	20	-4,1	3,4
			W (cm/s)	-19,7	17,9	-0,3	1,1
			Echo average (cnt)	43	130,4	51,6	3,1
GEOSTAR-SN3	2003-2004	CTD	T (°C)	13,52	13,61	13,54	0
			C (S/m)	4,631	4,697	4,681	0,007
			Depth (dbar)	3401,2	3401,9	3401,6	0,1
		Transmissometer	Beam attenuation (m^{-1})	0,344	0,398	0,363	0,015
		Current meter	U (cm/s)	-6,8	16,9	1,7	1,6
			V (cm/s)	-13,2	14,4	2,3	1,8
			W (cm/s)	-18,3	15,8	-0,9	1,3
		ADCP	U (cm/s)	-27,4	28,6	-1,6	4,6
			V (cm/s)	-29,9	23,3	0,1	2,5
			W (cm/s)	-23,4	7,4	-0,7	0,7
			Echo average (cnt)	43,2	59,8	44,1	0,6
	2004-2005	CTD	T (°C)	13,53	13,55	13,54	0,01
			C (S/m)	4,661	4,671	4,666	0,003
			Depth (dbar)	3401,2	3401,9	3401,6	0,1
		Transmissometer	Beam attenuation (m^{-1})	-0,072	0,008	-0,051	0,02
		Current meter	U (cm/s)	-15,9	16,4	1,2	1,4
			V (cm/s)	-15,9	19,8	2,3	1,7
			W (cm/s)	-17,2	15,4	-1,3	1
		ADCP	U (cm/s)	-19,4	19,9	0,4	3,2
			V (cm/s)	-19,5	20	-0,8	0,6
			W (cm/s)	-8,7	9,1	-0,7	0,6
			Echo average (cnt)	42,6	45,3	43,5	0,3

https://doi.org/10.5194/essd-2025-739
Preprint. Discussion started: 29 December 2025

Observatory name	Acquisition campaign	Sensor	Variable	Minimum	Maximum	Mean	Standard deviation
GEOSTAR	2007-2008	CTD	T (°C)	2,44	2,68	2,58	0,04
			C (S/m)	3,244	3,267	3,258	0,004
			Depth (dbar)	3254,3	3257,8	3256	0,8
		Turbidimeter	Turbidity (NTU)	-0,095	0,631	-0,017	0,037
		Current meter	U (cm/s)	-18,3	10,2	-0,3	2,2
			V (cm/s)	-15,7	17,3	-2	2,6
			W (cm/s)	-9,1	14,9	-0,6	0,7
		ADCP	U (cm/s)	-29,1	28,1	-0,7	3,7
			V (cm/s)	-29,2	28,9	-1,7	3,6
			W (cm/s)	-9,1	10,6	-0,4	0,5
			Echo average (cnt)	44,6	49,1	46,3	1
	2009-2010	CTD	T (°C)	2,48	2,67	2,61	0,03
			C (S/m)	3,246	3,264	3,258	0,003
			Depth (dbar)	3227,6	3231,3	3229,4	0,8
		Turbidimeter	Turbidity (NTU)	-0,076	0,543	-0,023	0,039
		Current meter	U (cm/s)	-9	11,3	0,1	0,6
			V (cm/s)	-11,3	10	-0,6	0,5
			W (cm/s)	-12,4	19,1	0	0,2
		ADCP	U (cm/s)	-29,6	28,5	-0,8	4,1
			V (cm/s)	-29	29,8	0,1	3,7
			W (cm/s)	-8,1	11,7	-0,5	0,5
			Echo average (cnt)	44,7	52,3	47,1	1,6
SN4	2009-2010	CTD	T (°C)	14,42	15,83	14,66	0,15
			C (S/m)	4,637	4,798	4,665	0,017
			Depth (dbar)	166,5	167,2	166,9	0,1
		Turbidimeter	Turbidity (NTU)	0,923	48,398	3,719	4,083
		Current meter	U (cm/s)	-39,4	26,6	-1,5	4,4
			V (cm/s)	-29,1	25,3	-0,4	2,3
			W (cm/s)	-29	11,9	-0,4	1,3
		Oxygen meter	O_2 (µmol/l)	5,1	103,1	39,1	9,2
	2013-2014	CTD	T (°C)	14,49	15,76	14,81	0,16
			C (S/m)	4,647	4,791	4,685	0,018
			Depth (dbar)	167,1	167,6	167,3	0,1
		Turbidimeter	Turbidity (NTU)	0,712	82,346	4,447	7,433
		Current meter	U (cm/s)	-30,9	6,2	-1,4	3,7
			V (cm/s)	-15,7	9,4	0,2	2,1
			W (cm/s)	-1,6	4,9	0,3	0,6

https://doi.org/10.5194/essd-2025-739
Preprint. Discussion started: 29 December 2025

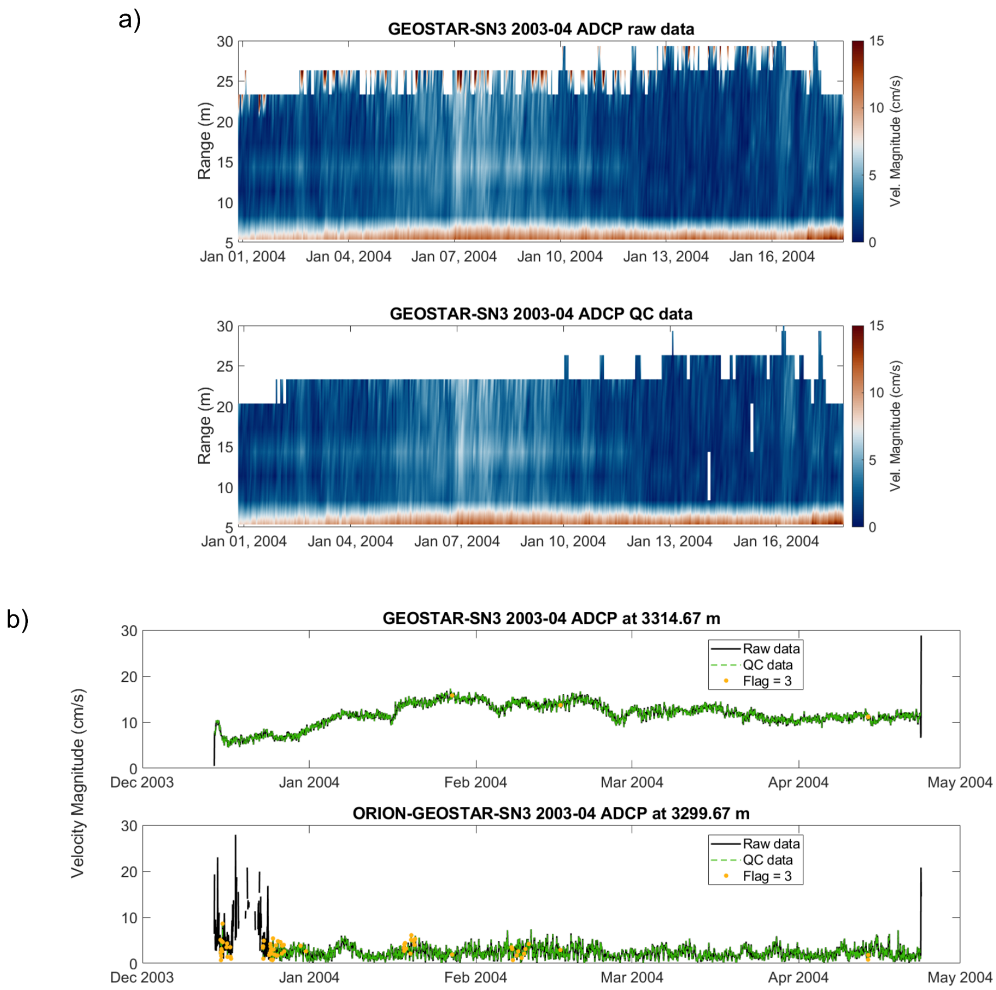

Figure 6: Quality control of ADCP velocity magnitude data at GEOSTAR-SN3 (2003–2004). (a) Color map of current magnitude across depth for January: top panel = raw data; bottom = QC-checked. (b) Time series from two depth bins (5.33 m on the top panel and 20.33 m bottom panel): black = raw, green = quality-checked, yellow = flagged.

4 Results

Although the acquired datasets pertain to several EOVs, the results reported here primarily concern temperature data, intending to provide some benchmarks of the deep layer state over the last decade across the Mediterranean Sea, from the Sea of Marmara to the Cádiz area. After post-processing a QC validation routine has been performed, potential temperature and density anomaly data derived following TEOS-10

https://doi.org/10.5194/essd-2025-739
Preprint. Discussion started: 29 December 2025

international standards (https://teos-10.org/), exhibit interesting variability at all sea-bottom sites monitored during these years (Figure 7).

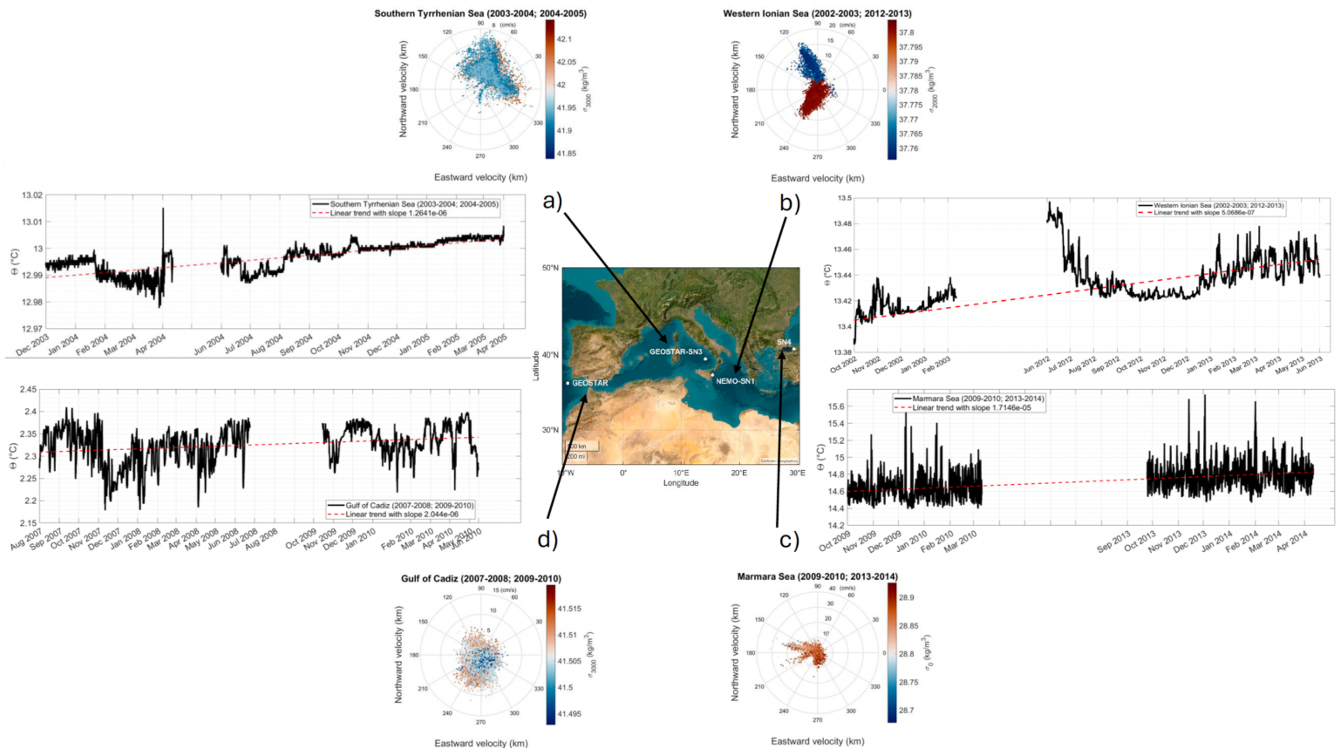

Figure 7: Temperature time series and corresponding current hodographs, along with potential density anomalies (calculated relative to in situ pressure), reveal a warming trend and variability observed in the Tyrrhenian Sea (a), the Ionian Sea (b), the Marmara Sea (c), and the Gulf of Cádiz (d) across the Mediterranean region (map at the center © *2025 Google Earth*).

Temperature trends measured between 2002 and 2013 at all monitored deep sites are consistently positive, in agreement with the global warming trend reported by the Intergovernmental Panel on Climate Change (*IPCC, 2013*). Although the statistical weight varies among sites depending on the length of the observation period, the annual rate of temperature increase, calculated for all datasets using least-squares linear fits to hourly measurements, remains within the same order of magnitude, ranging from +0.011 °C year^{-1} in the Tyrrhenian Sea to +0.018 °C year^{-1} in the Gulf of Cadiz and +0.047 °C year^{-1} in the Ionian Sea. The higher value observed in the Ionian Sea reflects the fact that it was derived from two time series collected a decade apart, providing a coherent and reliable estimate of a decadal-scale warming process.

The only exception is the Marmara Sea, where the rate is an order of magnitude higher (+0.15 °C year^{-1}), likely due to its shallower depth (166 m).
At all sites, temperature data reveal notable internal variability, but the recorded variations are not directly comparable as they result from differences in monitoring periods and local characteristics; therefore, they have to be assessed on a case-by-case basis. As for the NEMO-SN1 case in the Ionian Sea, where the variability recorded over one decade is not a simple warming signature but a real change of the deep-water masses (*Malanotte-Rizzoli et al., 1999; Hainbucher et al*., *2006*; *Artale et al. 2018*). This is evident looking at the current hodograph, also showing potential density anomaly (σ^2, calculated with reference pressure of 2000 dbar) (Figure 7b). In ten years, it reveals a change of $\Delta\sigma^2 = 0.05$ kg/m^3, which is four times bigger than the usual range of inter-annual variability expected at these depths in the Ionian bottom water. Along with changes in thermohaline properties, the current hodograph for the Ionian Sea also reveals a clear shift in the direction of prevailing currents (*Giambenedetti et al., 2024*), offering a rare snapshot of water mass redistribution. This shift may be attributed to the alternating advection of dense water masses that the Ionian basin receives from the Adriatic or Aegean Sea, which could sustain the better-known decadal reversals (BIOS) occurring in the upper-layer circulation (*Gacic et al., 2010*). This is an example of how the variability of the deep layer, generally assumed to be a stationary state environment, can instead feed internal processes impacting properties of the water masses and circulation dynamics.
Despite their scientific importance, deep-ocean time series remain sparse in both time and space. Therefore, developing techniques to handle data gaps and maximize the information content of existing records is essential. All time series here reported contain missing data, with gap lengths varying according to maintenance needs, technological refurbishments, or ship availability. To address these discontinuities, a combination of Singular Spectrum Analysis (SSA) and Optimal Interpolation (OI) was applied to selected time-series (Figure 8), demonstrating an effective approach to mitigate data gaps and fully exploit the available observations.
SSA is a fully data-driven, nonparametric method particularly suitable for time series with relatively long and continuous gaps, as it does not require a priori assumptions that might introduce artificial oscillations (*Ghil et al., 2002; Kondrashov and Ghil, 2006; Beckers and Rixen, 2003*). The approach involves two main steps: (i) SSA extracts the dominant deterministic components, such as trends, seasonal and tidal oscillations, and low-frequency variability, providing a continuous background estimate across missing intervals; and (ii) OI is then applied to the detrended and SSA-backgrounded residuals, optimally merging observed data with the reconstructed background field based on their covariance structure.
This SSA–OI approach combines the signal reconstruction capability of SSA with the statistical optimality of OI, effectively filling both short and long gaps while preserving the realistic variance and

https://doi.org/10.5194/essd-2025-739
Preprint. Discussion started: 29 December 2025

Open Access Earth System Science Data Discussions

autocorrelation structure of the original record. Through this process, missing segments were reconstructed by identifying and interpolating the dominant modes (6 mode) associated with physical oceanographic variability, thereby ensuring the temporal coherence and dynamical consistency of the reconstructed time series. Beyond data reconstruction, this approach enhances the performance of subsequent analyses, such as Power Spectral Density (PSD) estimation. As shown in Figure 8, the warming signal in the reconstructed time series (Figure 8, left part) is consistent with its spectral counterpart (Figure 8, right part). The alignment of the observed signal (black line) within the 95% confidence band (red line) confirms the robustness of the spectral estimate. Focusing on the deep-water component, both spectra display dominant energy at low frequencies, reflecting the slow and persistent variability typical of long-term warming processes evident in the reconstructed series. Distinct peaks at tidal and inertial frequencies are also apparent, though with different amplitudes, indicating that these processes remain active even at great depth and may contribute to the redistribution of accumulated thermal energy.

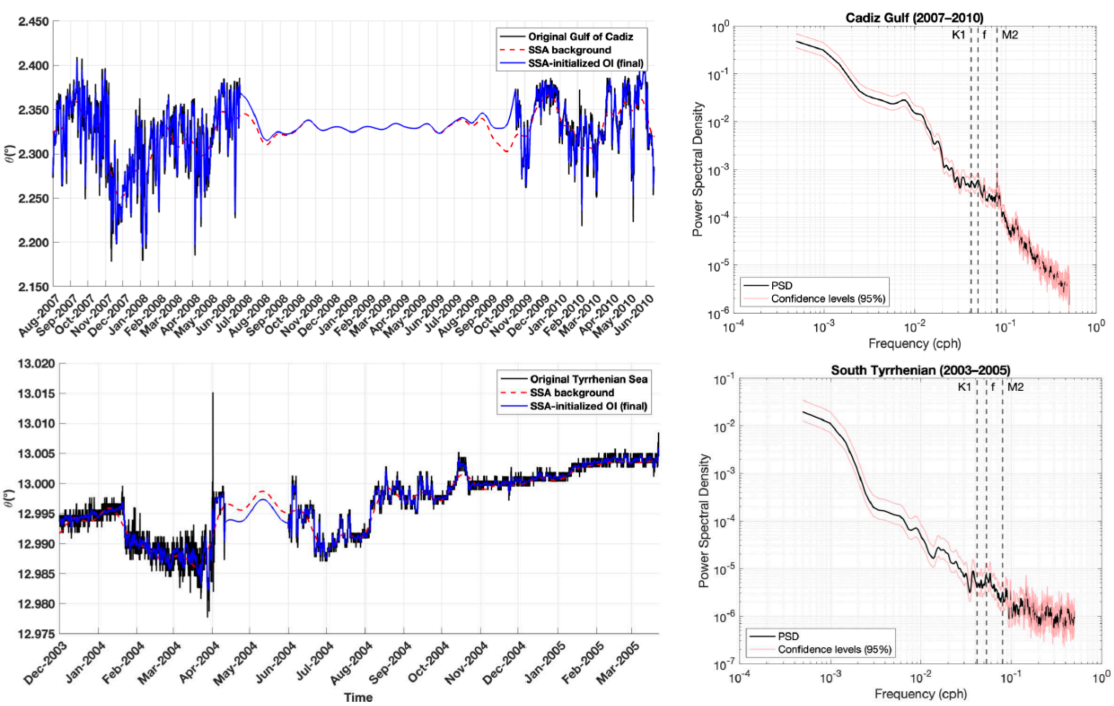

Figure 8. Time series from the Gulf of Cádiz (upper left) and the Tyrrhenian Sea (lower left) showing original data with gaps (black), SSA-based background estimation (red dashed line), and the reconstructed signal (blue line). Corresponding spectra (upper and lower right) highlight dominant low-frequency energy, indicating slow, persistent variability associated with long-term warming recorded.

https://doi.org/10.5194/essd-2025-739
Preprint. Discussion started: 29 December 2025

5 Data availability

The datasets described in this study can be accessed through the Multidisciplinary Oceanic Information SysTem (MOIST, https://doi.org/10.13127/MD/MOIST, *Azzarone et al., 2010*) and via the INGV ERDDAP server (http://oceano.bo.ingv.it/erddap/index.html), (Table 5 in Appendix A provides the complete references for each dataset.). Data and metadata have been formatted into NetCDF (Network Common Data Form) and comply with Climate and Forecasting (CF) metadata conventions. These specifications are also aligned with OceanSITES and SeaDataNet vocabularies, ensuring semantic clarity, long-term interoperability, and machine-readability. Domain-specific metadata attributes are harmonized using the NERC Vocabulary Server (NVS), which provides authoritative controlled vocabularies for parameter descriptions, units, and semantic consistency across datasets. Organizational identifiers follow the European Directory of Marine Organisations (EDMO) and the Research Organization Registry (ROR), and SPDX is used for licensing. In line with the INGV Data Policy, all datasets are released under a Creative Commons Attribution 4.0 International License (CC BY 4.0), allowing free use with appropriate citation. To be fully compliant with FAIR principles, each dataset is registered and assigned a Digital Object Identifier (DOI) through the INGV Data Registry (https://data.ingv.it/), acknowledging the efforts of those who contributed to generating the data and products and assuring data availability in further scientific publications. Multiple datasets are available, each corresponding to a specific observatory and mission. A comprehensive summary, including DOIs and citation formats, is available on the MOIST portal for each dataset.

6 Conclusions and Perspectives

The implementation of harmonized post-processing and quality control (QC) procedures for deep-sea data is a key step toward expanding the availability of reliable, high-quality oceanographic observations from the least sampled regions of the global ocean. Standardizing these methods ensures data accuracy and consistency while enabling the effective use and sharing of information essential to understanding deep-sea variability, still among the most poorly characterized components of the climate system. Beyond data collection, the application of advanced analytical methods proposed in this study minimizes spectral leakage and enhances the reliability of frequency-domain diagnostics, enabling a more accurate characterization of dominant variability modes and periodic signals. Furthermore, the reconstruction of longer and more continuous records increases the resolution and robustness of spectral estimates, allowing

https://doi.org/10.5194/essd-2025-739
Preprint. Discussion started: 29 December 2025

a deeper and more comprehensive interpretation of the frequencies associated with the observed oceanographic processes.

Strengthening and extending the deep-ocean observational network, particularly in under-sampled regions, remains essential to improve both regional process understanding and global climate modeling. By promoting open access and adherence to FAIR data principles, this effort contributes to the goals of the UN Decade of Ocean Science, supporting the development of a more integrated, sustainable, and climate-relevant deep-ocean observing framework.

https://doi.org/10.5194/essd-2025-739
Preprint. Discussion started: 29 December 2025

Open Access Earth System Science Data Discussions

Appendix A

Table 5: Summary of all datasets discussed in the paper, including their DOIs and corresponding citations

Observatory Name and acquisition period	Sensor type	Citation to add in the references
NEMO-SN1 (2002-2003)	CTD	Favali P., Beranzoli L., Etiope G., Marinaro G., Giambenedetti B., Lo Bue N.. CTD dataset with Quality Control (SBE 37-SM @ 1 sample / 12 min) from INGV/NEMO-SN1 seafloor platform during GNDT-SN1 project in Western Ionian Sea site (East Sicily), part of EMSO network. Istituto Nazionale di Geofisica e Vulcanologia (INGV). https://doi.org/10.13127/md/wis-sn1-2002-cdt-qc, 2024
	Current meter	Favali P., Beranzoli L., Etiope G., Marinaro G., Lo Bue N., Giambenedetti B.. Current meter dataset with Quality Control (FSI 3D-ACM @ 2 Hz) from INGV/SN1 seafloor platform during GNDT-SN1 project in Western Ionian Sea site (East Sicily), part of EMSO network. Istituto Nazionale di Geofisica e Vulcanologia (INGV). https://doi.org/10.13127/md/wis-sn1-2002-curr-qc, 2024
NEMO-SN1 (2012-2013)	CTD	Embriaco D., Marinaro G., Giovanetti G., Lo Bue N., Giambenedetti B.. CTD dataset with Quality Control (SBE 37-SM @ 1 sample / hour) from INGV/NEMO-SN1 seafloor platform during SMO project in Western Ionian Sea site (East Sicily), part of EMSO network. Istituto Nazionale di Geofisica e Vulcanologia (INGV). https://doi.org/10.13127/md/wis-sn1-2012-ctd-qc, 2023
	Current meter	Giovanetti G., Marinaro G., Embriaco D., Lo Bue N., Giambenedetti B.. Current meter dataset with Quality Control (Nobska MAVS-3 @ 2 Hz) from INGV/NEMO-SN1 seafloor platform during SMO project in Western Ionian Sea site (East Sicily), part of EMSO network. Istituto Nazionale di Geofisica e Vulcanologia (INGV). https://doi.org/10.13127/md/wis-sn1-2012-current_meter-qc, 2023
	ADCP	Giovanetti G., Marinaro G., Embriaco D., Lo Bue N., Giambenedetti B.. ADCP dataset with Quality Control (RDI WorkHorse 600 KHz @ 2 profile / hour) from INGV/NEMO-SN1 seafloor platform during SMO project in Western Ionian Sea site (East Sicily), part of EMSO network. Istituto Nazionale di Geofisica e Vulcanologia (INGV). https://doi.org/10.13127/md/wis-sn1-2012-adcp-qc, 2023
GEOSTAR SN3 (2003-2004)	CTD	Favali P., Beranzoli L., Etiope G., Marinaro G., Lo Bue N., Giambenedetti B. (2024). CTD dataset with Quality Control (SBE 16 @ 1 sample / hour) from INGV/GEOSTAR - SN-3 seafloor platform during ORION-GEOSTAR3 project in Southern Tyrrhenian Sea site (Marsili Basin), ORION1 campaign. Istituto Nazionale di Geofisica e Vulcanologia (INGV). https://doi.org/10.13127/md/sts-geostar-2003-ctd-qc, 2024
	Transmissometer	Favali P., Beranzoli L., Etiope G., Marinaro G., Lo Bue N., Giambenedetti B.. Transmissometer dataset with Quality Control (Ctg Alphatracka II @ 1 sample / hour) from INGV/GEOSTAR - SN-3 seafloor platform during ORION-GEOSTAR3 project in Southern Tyrrhenian Sea site (Marsili Basin), part of ORION network. Istituto Nazionale di Geofisica e Vulcanologia (INGV). https://doi.org/10.13127/md/sts-geostar-2003-transm-qc
	Current meter	Favali P., Beranzoli L., Etiope G., Marinaro G., Lo Bue N., Giambenedetti B.. Current meter dataset with Quality Control (FSI 3D-ACM @ 2 Hz) from INGV/GEOSTAR - SN-3 seafloor platform during ORION-GEOSTAR3 project in Southern Tyrrhenian Sea site (Marsili Basin), part of ORION network. Istituto Nazionale di Geofisica e Vulcanologia (INGV). https://doi.org/10.13127/md/sts-geostar-2003-curr-qc, 2024
	ADCP	Favali P., Beranzoli L., Etiope G., Marinaro G., Lo Bue N., Giambenedetti B.. ADCP dataset with Quality Control (RDI WorkHorse 300 kHz @ 1 sample / hour) from INGV/GEOSTAR - SN-3 seafloor platform during ORION-GEOSTAR3 project in Southern Tyrrhenian Sea site (Marsili Basin), part of ORION network. Istituto Nazionale di Geofisica e Vulcanologia (INGV). https://doi.org/10.13127/md/sts-geostar-2003-adcp-qc, 2024
GEOSTAR SN3 (2004-2005)	CTD	Favali P., Beranzoli L., Etiope G., Marinaro G., Lo Bue N., Giambenedetti B.. CTD dataset with Quality Control (SBE 16 @ 1 sample / hour) from INGV/GEOSTAR - SN-3 seafloor platform during ORION-GEOSTAR3 project in Southern Tyrrhenian Sea site (Marsili Basin), ORION2 campaign. Istituto Nazionale di Geofisica e Vulcanologia (INGV). https://doi.org/10.13127/md/sts-geostar-2004-ctd-qc, 2024
	Transmissometer	Favali P., Beranzoli L., Etiope G., Marinaro G., Lo Bue N., Giambenedetti B.. Transmissometer dataset (alphatracka II @ 1 sample / hour) from INGV/GEOSTAR - SN-3 seafloor platform during ORION-GEOSTAR3 project in Southern Tyrrhenian Sea site (Marsili Basin), part of ORION network. Istituto Nazionale di Geofisica e Vulcanologia (INGV). https://doi.org/10.13127/md/sts-geostar-2004-transm-qc, 2024
	Current meter	Favali P., Beranzoli L., Etiope G., Marinaro G., Lo Bue N., Giambenedetti B.. Current meter dataset with Quality Control (FSI 3D-ACM @ 2 Hz) from INGV/GEOSTAR - SN-3 seafloor platform during ORION-GEOSTAR3 project in Southern Tyrrhenian Sea site (Marsili Basin), part of ORION network. Istituto Nazionale di Geofisica e Vulcanologia (INGV). https://doi.org/10.13127/md/sts-geostar-2004-curr-qc, 2024
	ADCP	Favali P., Beranzoli L., Etiope G., Marinaro G., Lo Bue N., Giambenedetti B.. ADCP dataset with Quality Control (RDI WorkHorse 300 KHz @ 1 profile / hour) from INGV/GEOSTAR - SN-3 seafloor platform during ORION-GEOSTAR3 project in Southern Tyrrhenian Sea site (Marsili Basin), part of ORION network. Istituto Nazionale di Geofisica e Vulcanologia (INGV). https://doi.org/10.13127/md/sts-geostar-2004-adcp, 2024

https://doi.org/10.5194/essd-2025-739
Preprint. Discussion started: 29 December 2025

Open Access Earth System Science Data Discussions

GEOSTAR (2007-2008)	CTD	Lo Bue N., Giambenedetti B.. CTD dataset with Quality Control (SBE 16plus @ 1 sample / hour) from INGV/GEOSTAR seafloor platform during NEAREST project in Iberian Margin site (Gulf of Cadiz), part of EMSO network. Istituto Nazionale di Geofisica e Vulcanologia (INGV). https://doi.org/10.13127/md/im-geostar-2007-ctd-qc, 2023
	Turbidity meter	Marinaro G., Embriaco D., Lo Bue N., Giambenedetti B.. Turbidity meter dataset with Quality Control (ECO-BB(RT)D 6000m @ 1 sample / hour) from INGV/GEOSTAR seafloor platform during NEAREST project in Iberian Margin site (Gulf of Cadiz), part of EMSO network. Istituto Nazionale di Geofisica e Vulcanologia (INGV). https://doi.org/10.13127/md/im-geostar-2007-turb-qc, 2023
	Current meter	Marinaro G., Embriaco D., Lo Bue N., Giambenedetti B.. Current meter dataset with Quality Control (Nobska MAVS-3 @ 5 Hz) from INGV/GEOSTAR seafloor platform during NEAREST project in Iberian Margin site (Gulf of Cadiz), part of EMSO network. Istituto Nazionale di Geofisica e Vulcanologia (INGV). https://doi.org/10.13127/md/im-geostar-2007-curr-qc, 2023
	ADCP	Marinaro G., Embriaco D., Lo Bue N., Giambenedetti B.. ADCP dataset with Quality Control (RDI WorkHorse 300 kHz @ 1 profile / hour) from INGV/GEOSTAR seafloor platform during NEAREST project in Iberian Margin site (Gulf of Cadiz), part of EMSO network. Istituto Nazionale di Geofisica e Vulcanologia (INGV). https://doi.org/10.13127/md/im-geostar-2007-adcp-qc, 2023
GEOSTAR (2009-2010)	CTD	Embriaco D., Marinaro G., Lo Bue N., Giambenedetti B.. CTD dataset with Quality Control (SBE 16plus @ 1 sample / hour) from INGV/GEOSTAR seafloor platform during Esonet NoE project in Iberian Margin site (Gulf of Cadiz), part of EMSO network. Istituto Nazionale di Geofisica e Vulcanologia (INGV). https://doi.org/10.13127/md/im-geostar-2009-ctd-qc,2023
	Turbidity meter	Embriaco D., Marinaro G., Lo Bue N., Giambenedetti B.. CTD dataset with Quality Control (SBE 16plus @ 1 sample / hour) from INGV/GEOSTAR seafloor platform during Esonet NoE project in Iberian Margin site (Gulf of Cadiz), part of EMSO network. Istituto Nazionale di Geofisica e Vulcanologia (INGV). https://doi.org/10.13127/md/im-geostar-2009-ctd-qc,2023
	Current meter	Embriaco D., Marinaro G., Lo Bue N., Giambenedetti B.. Current meter dataset with Quality Control (Nobska MAVS-3 @ 5 Hz) from INGV/GEOSTAR seafloor platform during Esonet NoE project in Iberian Margin site (Gulf of Cadiz), part of EMSO network. Istituto Nazionale di Geofisica e Vulcanologia (INGV). https://doi.org/10.13127/md/im-geostar-2009-curr-qc, 2023
	ADCP	Embriaco D., Marinaro G., Lo Bue N., Giambenedetti B.. ADCP dataset with Quality Control (RDI WorkHorse 300 kHz @ 1 sample / hour) from INGV/GEOSTAR seafloor platform during ESONET-NOE-LIDO project in Iberian Margin site (Gulf of Cadiz), part of EMSO network. Istituto Nazionale di Geofisica e Vulcanologia (INGV). https://doi.org/10.13127/md/im-geostar-2009-adcp-qc, 2023
SN4 (2009-2010)	CTD	Marinaro G., Embriaco D., Lo Bue N., Giambenedetti B.. CTD dataset with Quality Control (SBE 16plus @ 1 sample / 10 min) from INGV/SN-4 seafloor platform during ESONET-MARMARA-DM project in Marmara Sea site (Marmara Sea), part of EMSO network. Istituto Nazionale di Geofisica e Vulcanologia (INGV). https://doi.org/10.13127/md/mar-sn4-2009-ctd-qc, 2024
	Turbidity meter	Marinaro G., Embriaco D., Lo Bue N., Giambenedetti B.. Turbidity meter dataset with Quality Control (ECO-NTU(RT)D 6000m @ 1 sample / 10 min) from INGV/SN-4 seafloor platform during ESONET-MARMARA-DM project in Marmara Sea site (Marmara Sea), part of EMSO network. Istituto Nazionale di Geofisica e Vulcanologia (INGV). https://doi.org/10.13127/md/mar-sn4-2009-turb-qc, 2024
	Current meter	Marinaro G., Embriaco D., Lo Bue N., Giambenedetti B.. Current meter dataset with Quality Control (Nobska MAVS-3 @ 5 Hz) from INGV/SN-4 seafloor platform during ESONET-MARMARA-DM project in Marmara Sea site (Marmara Sea), part of EMSO network. Istituto Nazionale di Geofisica e Vulcanologia (INGV). https://doi.org/10.13127/md/mar-sn4-2009-curr-qc, 2024
	Oxygen	Marinaro G., Lo Bue N., Giambenedetti B.. Oxygen meter dataset with Quality Control (AADI Optode 3830 @ 1 Hz) from INGV/SN-4 seafloor platform during ESONET-MARMARA-DM project in Marmara Sea site (Marmara Sea), part of EMSO network. Istituto Nazionale di Geofisica e Vulcanologia (INGV). https://doi.org/10.13127/md/ms-sn4-2009-oxygen_meter-qc, 2024
SN4 (2013-2014)	CTD	Marinaro G., Embriaco D., Lo Bue N., Giambenedetti B.. CTD dataset with Quality Control (SBE 16plus @ 1 sample / hour) from INGV/SN-4 seafloor platform during MARSITE 1 project in Marmara Sea site (Marmara Sea), part of EMSO network. Istituto Nazionale di Geofisica e Vulcanologia (INGV). https://doi.org/10.13127/md/mar-sn4-2013-ctd-qc, 2024
	Turbidity meter	Marinaro G., Embriaco D., Lo Bue N., Giambenedetti B.Turbidity meter dataset with Quality Control (ECO-NTU(RT)D 6000m @ 1 sample / 10 min) from INGV/SN-4 seafloor platform during MARSITE 1 project in Marmara Sea site (Marmara Sea), part of EMSO network. Istituto Nazionale di Geofisica e Vulcanologia (INGV). https://doi.org/10.13127/md/mar-sn4-2013-turb-qc, 2024
	Current meter	Marinaro G., Embriaco D., Lo Bue N., Giambenedetti B.. Current meter dataset with Quality Control (Nobska MAVS-3 @ 5 Hz) from INGV/SN-4 seafloor platform during MARSITE 1 project in Marmara Sea site (Marmara Sea), part of EMSO network. Istituto Nazionale di Geofisica e Vulcanologia (INGV). https://doi.org/10.13127/md/mar-sn4-2013-curr-qc, 2024

Author contributions. Concept development and manuscript writing were carried out by NLB and BG, with input from all co-authors. Measurements were performed by NLB and GM. Data processing and analysis were conducted by NLB and BG, while data curation was handled by BG, DE, PB, CF, and RV. All authors have read and approved the final version of the manuscript.

Competing interest. The authors declare that they have no conflict of interest.

https://doi.org/10.5194/essd-2025-739
Preprint. Discussion started: 29 December 2025

Acknowledgments. We wish to express our gratitude to all those who, over the past 30 years, have contributed to the development of deep-sea observatory technology from the preparation and management of several EC projects that enabled their creation, to their design, construction, and deployment at sea. This achievement was made possible through the combined efforts of numerous researchers, engineers, and technicians, all united by a shared spirit of experimentation and scientific curiosity.

Financial support. This study was developed and financially supported within the framework of the INGV departmental project MACMAP.

References

1. **Alves, J. M. R., Carton, X., and Ambar, I.** (2011): Hydrological structure, circulation and water mass transport in the Gulf of Cadiz, *Int. J. Geosci.*, **2**, 432–456, https://doi.org/10.4236/ijg.2011.24047.
2. **Artale, V., et al.** (2018): Linking mixing processes and climate variability to the heat content distribution of the Eastern Mediterranean abyss, *Sci. Rep.*, **8**, 11317, https://doi.org/10.1038/s41598-018-29343-4.
3. **Azzarone, A., Marcucci, N. M., & Marinaro, G.** (2010). Multidisciplinary Oceanic Information SysTem (MOIST). Istituto Nazionale di Geofisica e Vulcanologia (INGV). https://doi.org/10.13127/MD/MOIST
4. **Beckers, J. M. and Rixen, M.** (2003): EOF calculations and data filling from incomplete oceanographic datasets, *J. Atmos. Oceanic Technol.*, **20**, 1839–1856, https://doi.org/10.1175/1520-0426(2003)020<1839:ECADFF>2.0.CO;2.
5. **Beranzoli, L., De Santis, A., Etiope, G., Favali, P., Frugoni, F., Smriglio, G., Gasparoni, F., and Marigo, A.** (1998): GEOSTAR: a geophysical and oceanographic station for abyssal research, *Phys. Earth Planet. Inter.*, **108**, 175–183, https://doi.org/10.1016/S0031-9201(98)00094-6.
6. **Beranzoli, L., De Santis, A., Calcara, M., Ciafardini, A., et al.** (2009): Multiparametric seafloor exploration: the Marsili Basin and volcanic seamount case (Tyrrhenian Sea, Italy), in: *Proc. 3rd IASME/WSEAS Int. Conf. Geology and Seismology (GES'09)*, WSEAS Press.
7. **Budillon, G., Lo Bue, N., Siena, G., and Spezie, G.** (2010): Hydrographic characteristics of water masses and circulation in the Northern Ionian Sea, *Deep Sea Res. II*, **57**, 441–457, https://doi.org/10.1016/j.dsr2.2009.08.017.
8. **Bushnell, M., Waldmann, C., Seitz, S., Buckley, E., Tamburri, M., Hermes, J., et al.** (2019): Quality assurance of oceanographic observations: standards and guidance adopted by an international partnership, *Front. Mar. Sci.*, **6**, 706, https://doi.org/10.3389/fmars.2019.00706.
9. **de Lavergne, C., Madec, G., Capet, X., et al.** (2016): Getting to the bottom of the ocean, *Nat. Geosci.*, **9**, 857–858, https://doi.org/10.1038/ngeo2850.
10. **Desbruyères, D. G., Purkey, S. G., McDonagh, E. L., Johnson, G. C., and King, B. A.** (2016): Deep and abyssal ocean warming from 35 years of repeat hydrography, *Geophys. Res. Lett.*, **43**, 10356–10365, https://doi.org/10.1002/2016GL070413.
11. **Embriaco, D., Marinaro, G., Frugoni, F., Monna, S., et al.** (2014): Monitoring of gas and seismic energy release along the North Anatolian Fault (Sea of Marmara, NW Turkey), *Geophys. J. Int.*, **196**, 850–866.
12. **Favali, P., Beranzoli, L., D'Anna, G., Gasparoni, F., et al.** (2006): NEMO-SN-1: the first real-time seafloor observatory of ESONET, *Nucl. Instrum. Methods Phys. Res. A*, **567**, 462–467.

13. **Favali, P., Beranzoli, L., D'Anna, G., Gasparoni, F., et al.** (2009): A fleet of multiparameter observatories for geophysical and environmental monitoring at seafloor, *Ann. Geophys.*, **49**.
14. **Favali, P., Beranzoli, L., Italiano, F., Migneco, E., et al.** (2011): NEMO-SN1 developments in view of the EMSO and KM3Net infrastructures, *Nucl. Instrum. Methods Phys. Res. A*, **626–627**, S53–S56.
15. **Favali, P., Chierici, F., Marinaro, G., Giovanetti, G., et al.** (2013): NEMO-SN1 cabled observatory in the Western Ionian Sea, *IEEE J. Oceanic Eng.*, **38**, 358–374.
16. **Ferrari, R., Mashayek, A., McDougall, T. J., Nikurashin, M., et al.** (2016): Turning ocean mixing upside down, *J. Phys. Oceanogr.*, **46**, 23–.
17. **Gačić, M., Borzelli, G. E., Civitarese, G., Cardin, V., et al.** (2010): Can internal processes sustain reversals of ocean upper circulation? The Ionian Sea example, *Geophys. Res. Lett.*, **37**, L09608, https://doi.org/10.1029/2010GL043216.
18. **García-Lafuente, J., Delgado, J., Criado-Aldeanueva, F., Bruno, M., et al.** (2006): Water mass circulation on the continental shelf of the Gulf of Cádiz, *Deep Sea Res. II*, **53**, 1182–1197, https://doi.org/10.1016/j.dsr2.2006.04.011.
19. **Giambenedetti, B., Lo Bue, N., and Artale, V.** (2024): Role of abyssal ocean stratification in potential vorticity redistribution through the water column, *Ocean Sci.*, **20**, 1209–1228, https://doi.org/10.5194/os-20-1209-2024.
20. **Giovanetti, G., Monna, S., Lo Bue, N., Embriaco, D., et al.** (2016): Observing volcanoes from the seafloor in the central Mediterranean area, *Remote Sens.*, **8**, 298, https://doi.org/10.3390/rs8040298.
21. **Hainbucher, D., Rubino, A., and Klein, B.** (2006): Water mass characteristics in the deep layers of the western Ionian Basin, *Geophys. Res. Lett.*, **33**, L05608, https://doi.org/10.1029/2005GL025318.
22. **Heuzé, C., Purkey, S. G., and Johnson, G. C.** (2022): It is high time we monitor the deep ocean, *Environ. Res. Lett.*, **17**, 121002.
23. **Howell, K. L., Hilário, A., Allcock, A. L., et al.** (2021): A decade to study deep-sea life, *Nat. Ecol. Evol.*, **5**, 265–267, https://doi.org/10.1038/s41559-020-01352-5.
24. **IOC, SCOR, and IAPSO** (2010): The international thermodynamic equation of seawater – 2010, *Manuals and Guides*, **56**, 196 pp.
25. **IPCC** (2013): Climate Change 2013: The Physical Science Basis, Cambridge University Press.
26. **Kondrashov, D. and Ghil, M.** (2006): Spatio-temporal filling of missing points in geophysical data sets, *Nonlin. Processes Geophys.*, **13**, 151–159, https://doi.org/10.5194/npg-13-151-2006.
27. **Lascaratos, A., Roether, W., Nittis, K., and Klein, B.** (1999): Recent changes in deep water formation and spreading in the eastern Mediterranean Sea, *Prog. Oceanogr.*, **44**, 5–36, https://doi.org/10.1016/S0079-6611(99)00019-1.
28. **Levin, L. A., Bett, B. J., Gates, A. R., Heimbach, P., et al.** (2019): Global observing needs in the deep ocean, *Front. Mar. Sci.*, **6**, 241, https://doi.org/10.3389/fmars.2019.00241.
29. **Lo Bue, N., Artale, V., and Schroeder, K.** (2021): Impact of deep oceanic processes on circulation and climate variability, *Front. Mar. Sci.*, **8**, 801479, https://doi.org/10.3389/fmars.2021.801479.
30. **MacDougall, T. J. and Barker, P. M.** (2011): Getting started with TEOS-10 and the GSW Oceanographic Toolbox, SCOR/IAPSO WG127, 28 pp.
31. **MacKinnon, J. A., Zhao, Z., Whalen, C. B., Waterhouse, A. F., et al.** (2017): Climate Process Team on internal wave–driven ocean mixing, *Bull. Am. Meteorol. Soc.*, **98**, 2429–2454.
32. **Malanotte-Rizzoli, P., Manca, B. B., d'Alcalà, M. R., Theocharis, A., et al.** (1997): Hydrography and circulation in the Ionian Sea during POEM-Phase I, *Prog. Oceanogr.*, **39**, 153–204.
33. **Malanotte-Rizzoli, P., Manca, B. B., d'Alcalà, M. R., Theocharis, A., et al.** (1999): The Eastern Mediterranean in the 80s and 90s: transition of intermediate and deep circulations, *Dyn. Atmos. Oceans*, **29**, 365–395.
34. **Marinaro, G., Etiope, G., Lo Bue, N., Favali, P., et al.** (2006): Monitoring of a methane-seeping pockmark by cabled benthic observatory, *Geo-Mar. Lett.*, **26**, 297–302.
35. **Munk, W.** (1966): Abyssal recipes, *Deep Sea Res.*, **13**, 707–730.

https://doi.org/10.5194/essd-2025-739
Preprint. Discussion started: 29 December 2025

36. **Ochoa, J. and Bray, N.** (1991): Water mass exchange in the Gulf of Cádiz, *Deep Sea Res. A*, **38**, S465–S503.
37. **Polzin, K. L. and McDougall, T.** (2021): Mixing at the ocean's bottom boundary, in: *Drivers, Mechanisms and Impacts*, Elsevier.
38. **Pouliquen, S., et al.** (2011): Recommendations for in-situ data real-time quality control.
39. **Rhein, M., Rintoul, S., Aoki, S., Campos, E., Chambers, D., Feely, R., and Wang, F.** (2013): Observations: Ocean, in *Climate Change 2013: The Physical Science Basis*, IPCC.
40. **Stommel, H. and Arons, A. B.** (1960): On the abyssal circulation of the world ocean–II, *Deep Sea Res.*, **6**, 217–233.
41. **Talley, L. D., Pickard, G. L., and Emery, W. J.** (2011): *Descriptive Physical Oceanography*, 6th ed., Academic Press.
42. **Visbeck, M.** (2018): Ocean science research is key for a sustainable future, *Nat. Commun.*, **9**, 690, https://doi.org/10.1038/s41467-018-03158-3.